Quantifying Precipitation Suppression Due to Air Pollution

AMIR GIVATI AND DANIEL ROSENFELD

The Hebrew University of Jerusalem, Jerusalem, Israel

(Manuscript received 3 August 2003, in final form 20 January 2004)

ABSTRACT

Urban air pollution and industrial air pollution have been shown qualitatively to suppress rain and snow. Here, precipitation losses over topographical barriers downwind of major coastal urban areas in California and in the land of Israel that amount to 15%–25% of the annual precipitation are quantified. The suppression occurs mainly in the relatively shallow orographic clouds within the cold air mass of cyclones. The suppression that occurs over the upslope side is coupled with similar percentage enhancement on the much drier downslope side of the hills. The evidence includes significant decreasing trends of the ratio of hill to coast precipitation during the twentieth century in polluted areas in line with the increasing emissions during the same period, whereas no trends are observed in similar nearby pristine areas. The evidence suggests that air-pollution aerosols that are incorporated in orographic clouds slow down cloud-drop coalescence and riming on ice precipitation and hence delay the conversion of cloud water into precipitation. This effect explains the pattern of greatest loss of precipitation at the midlevel of the upwind slopes, smaller losses at the crest, and enhancement at the downslope side of the hills.

1. Introduction

The objective of this study is the first-ever quantification of the microphysical effect of air-pollution aerosols on precipitation on a regional scale (tens to several hundreds of kilometers). Previous studies have shown qualitatively that urban and industrial air pollution suppresses precipitation-forming processes in convective clouds (Rosenfeld 1999, 2000). The pollution aerosols serve as small cloud condensation nuclei (CCN) that form large concentrations of small cloud droplets. This process in turn suppresses the drop coalescence and the warm-rain processes, as well as the ice precipitation (Rosenfeld 2000; Borys et al. 2003), and so prolongs the time required to convert the cloud water that exists in small drops into large hydrometeors that can precipitate. Borys et al. (2003) show that the addition of as little as 1 μg m^{-3} of anthropogenic sulfate aerosols to a clean background can reduce the orographic snowfall rate in the Colorado Rocky Mountains by up to 50%. The suppression is stronger in shallower clouds with warmer top temperatures. Satellite observations showed that pollution can completely shut off precipitation from clouds that have temperatures at their tops $>-10°$C (Rosenfeld and Woodley 2003). Therefore, one can expect to find the greatest rain suppression in regions that are dominated by relatively short-lived clouds with relatively warm tops downwind of major urban areas. Because of their short life, such clouds are more sensitive to the slowing down of the conversion of cloud water to precipitation, whereas long-lived clouds would eventually convert their water into precipitation regardless of the conversion rate. The urban heat island has been documented previously as the main cause for precipitation enhancement in the warm season downwind of major urban areas (Changnon 1979; Changnon et al. 1991; Shepherd et al. 2002). Therefore, we had to select regions in which the precipitation is dominated by clouds that are not thermally driven, preferably formed by orographic lifting over mountain ranges downwind of pollution sources during the cold season. We used annual rainfall data because almost all of the precipitation in the areas of interest occurs in the winter or in winterlike storms during the spring and autumn.

Corresponding author address: Daniel Rosenfeld, Institute of Earth Sciences, The Hebrew University of Jerusalem, Jerusalem 91904, Israel.
E-mail: daniel@vms.huji.ac.il

2. The study areas and data collection

In the ideal, the effect would be most pronounced downwind of coastal cities with hills inland that receive precipitation mainly during the winter in maritime onshore flow from shallow convective clouds. The main effect would be, therefore, the suppression of the orographic component of the precipitation, which would be manifested as a reduction in the orographic enhancement factor Ro, where Ro is defined as the ratio between the precipitation amounts at the hills and at the upwind lowland. Such conditions are abundant, especially on the west coast of continents in the subtropics and midlatitudes, where the precipitation over hills is a major source for the scarce water there. This study analyzes historical records of precipitation from California and from the land of Israel as representative of these conditions (see maps in Fig. 1).

The main analysis tool is the time series of Ro based on annual precipitation from rain gauges downwind and sidewind of major urban areas. The underlying assumption is that small-particulate air-pollution emissions have increased with the growth of urban areas, resulting in a decrease in Ro with time. The sidewind Ro time series are not expected to show any trend with time and so serve as controls.

3. Results and discussion

a. Trend analyses of rain gauges

Figures 2–5 display the longest annual time series that could be found in California and Israel for urban downwind and sidewind pairs of rain gauges. According to Fig. 2d, Ro decreased by 28% in the mountains to the east of San Diego, California, during the twentieth century, most of it after 1940 when San Diego started to grow, and more recently with the explosive growth of Tijuana just across the Mexican border. No such decrease could be detected farther north, midway between San Diego and Los Angeles, California, but a decrease has occurred again downwind of the Los Angeles (Fig. 6a), Fresno, California, and San Francisco, California, areas. Farther north, in the sparsely populated northern California, again no decreasing precipitation trends were observed (Fig. 3c). Furthermore, there were some statistically insignificant increases. A similar situation is evident in Israel (Figs. 4d, 5d). These trends occurred consistently in all of the pairs of rain gauges that were tested and are summarized in the tables in the appendix. The decreasing trend of Ro does not necessarily mean an absolute decrease of precipitation, because the precipitation decreases may have occurred in the context of long-term increases in the overall precipitation (see absolute trends in Figs. 2a, 2b, 3a, 3b, 4a, 4b, 5a, and 5b).

Many more rain gauges have been available for such trend analysis for the last 60 yr, making it possible to compare clusters of rain gauges in the hill and upwind plain areas. Their analysis shows a clear signal of decreasing Ro in the San Diego, Los Angeles, and San Francisco areas and in central Israel. Additional analyses of other areas in California and Israel (see the appendix) show that the decreasing trends occur at the western slopes of the hills that are located downwind of pollution sources. Again, such a trend was not found in hills downwind of pristine areas. The continuous decrease of Ro is consistent with the increasing trend of air pollution in Israel throughout the period. However, the values of standard air-quality measurements in California have improved since the late 1970s (Malm et al. 2002) while Ro continues to decrease at a somewhat lesser rate, as shown in the appendix. This pattern raises a question as to whether it is really the particulate air pollution that is responsible for the observed trends in Ro.

b. The radiosonde model

The most likely alternative explanation to the reduction in Ro is a decreasing trend in the cross-mountain component of the low-tropospheric wind velocity and moisture flux during rain events. Orographic precipitation has already been related quantitatively to the low-level winds and moisture in both California (Pandey et al. 1999; Neiman et al. 2002) and Israel (Alpert and Shafir 1991; Rosenfeld and Farbstein 1992). We applied the radiosonde regression model after Rosenfeld and Farbstein (1992) to predict the daily rain amounts in the hilly stations, where the upwind coastal precipitation and the cross-mountain 850-hPa wind velocity and the absolute humidity at that level are $RMM = RCM(WS \times W)$, where RMM is the predicted precipitation in the mountains (mm day^{-1}), RCM is the gauged precipitation at the coast (mm day^{-1}), WS is the wind speed component toward the mountain (m s^{-1}), and W is the mixing ratio (g kg^{-1}).

Radiosonde data have been available since the early 1950s for both California and Israel. The model results show that the ratio between the measured rain and the predicted rain (which is unaffected by pollution) for polluted mountain areas decreased in both California and Israel in a manner very similar to the observed trends of Ro. The model results for clean areas show no difference between the measured and predicted rain. In essence, this result reflects that the relevant meteorological conditions during rain days did not change systematically along the years, and the observed trends in Ro are likely caused by nonmeteorological reasons, such as anthropogenic air pollution.

c. Aerosol properties

In line with these considerations, despite the reported decreases in the pollutant emissions in California during the last two decades, the total amount of soluble pollution ions in precipitation particles aloft has not shown any decreasing trend and even showed a slight increasing trend in Sequoia National Park (Table 1). Therefore, the expectation for a recent recovery of Ro with the improving standards cannot be supported by these observations of the recent trend of steady to increasing concentrations of pollution in the precipitation. The contaminants in the precipitation were monitored in the Sierra Nevada at elevated locations that eliminated the possibility of scavenging the pollutants below cloud base, because the monitoring stations were mostly above cloud-base level during precipitation events. Local sources for pollutant species such as SO_2, NO_x, and NH_3 were found to be relatively unimportant in the Yo-

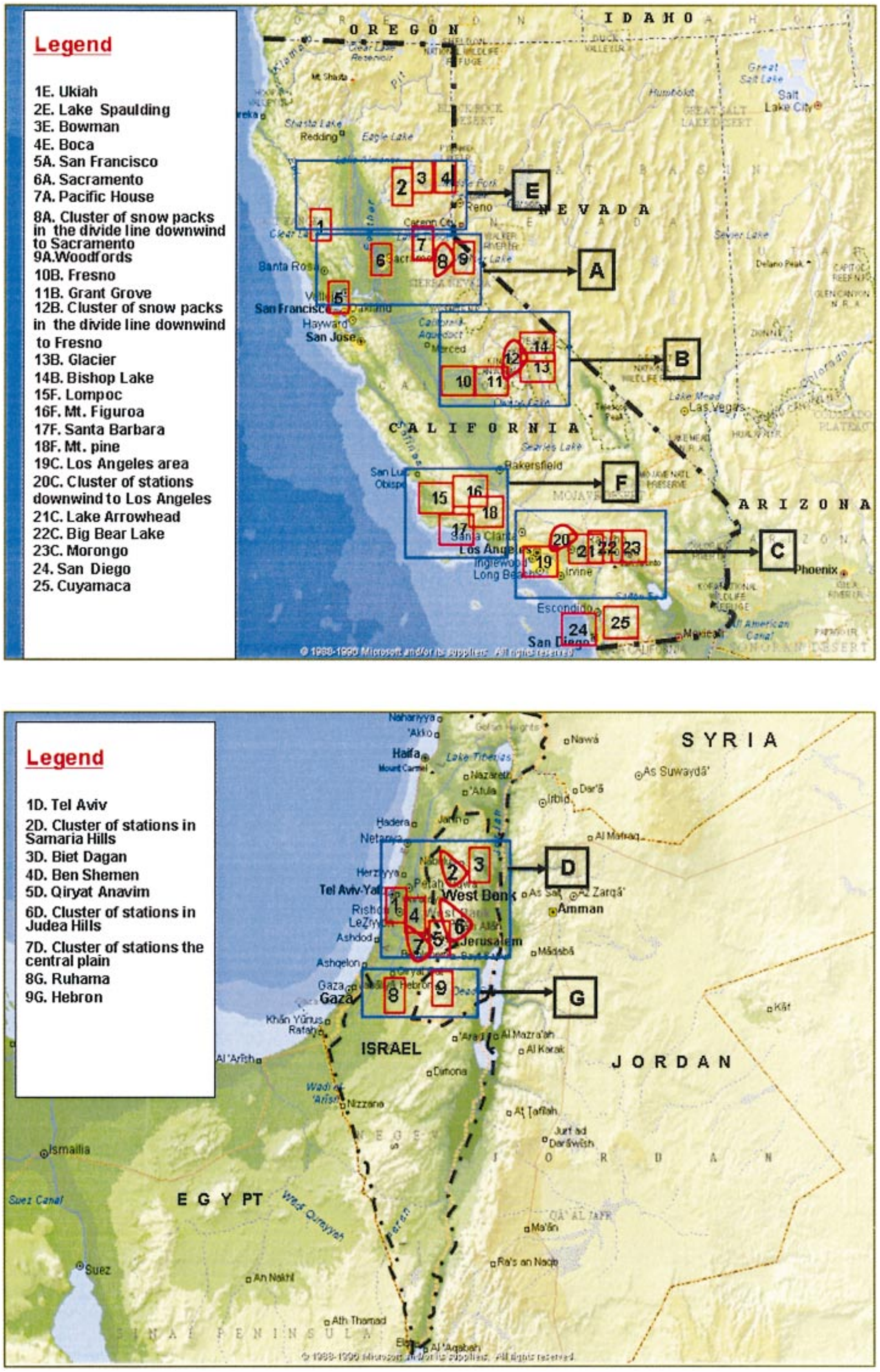

FIG. 1. Map of the rain gauge locations in (top) California and (bottom) Israel. The red rectangular frames represent the rain gauge locations, and the red irregular frames represent the cluster locations. The blue frames (A–G) represent different geographical areas. More details about those areas are given in Figs. 10 and 11.

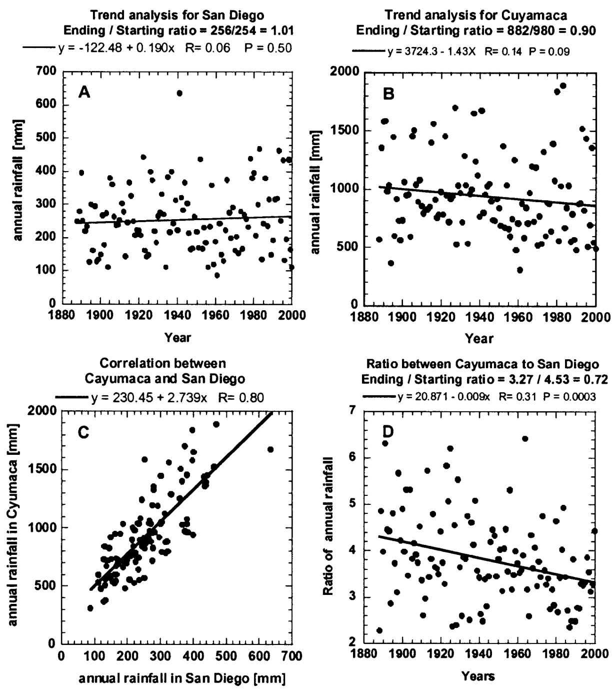

FIG. 2. Long-range trends of the annual precipitation measured in (a) San Diego and in (b) the downwind hilly station of Cuyamaca at an elevation of 1550 m, (c) the correlation between these two stations, and (d) the annual ratio of precipitation (Ro) measured between them. The stations with the longest record in California are presented here. Note the sharp decrease in Ro with time in this area, which is affected by urban air pollution. Ending/starting ratio is the ratio at the beginning of the time series divided by the ratio at the end, as calculated from the regression line at these times, *R* is the linear correlation coefficient, and *P* is the statistical significance that corresponds to the *t*-test statistic.

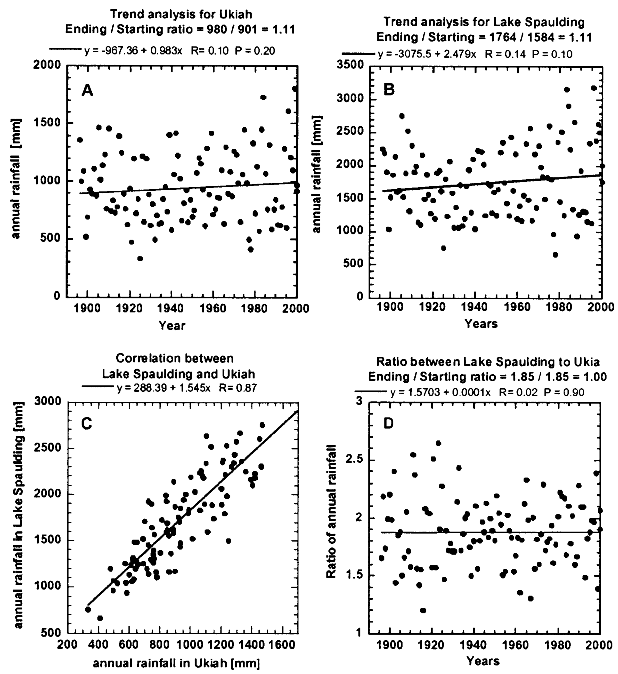

FIG. 3. Same as in Fig. 2, but for the relatively clean area in northern California at (a) Ukiah and (b) the downwind hilly station of Lake Spaulding at an elevation of 1717 m. (c) The annual precipitation of the two stations is correlated well. Both stations show increases in precipitation over the period of record. (d) Note the lack of a trend in the ratio between the hilly and upwind lowland stations.

semite and Sequoia National Parks and were attributed to transport from the urban areas and from the oil industry in the southern San Joaquin Valley (Collett 1989; Collett et al. 1989, 1990; Takemoto et al. 1995; Carroll and Dixon 2002). Indeed, the combined concentrations of non–sea salt ions in the precipitation (Ca, Mg, K, NH_4, NO_3, and SO_4) at the mountain stations of the Sierra Nevada, showing a significant decreasing trend of precipitation (Fig. 7), were 2 times the concentration found in the northern Sierra Nevada, where no trend in Ro is indicated (see Table 1). These ions, especially sulfates and nitrates, are major constituents of pollution-produced CCN particles.

d. Trend of very small CCN

A prime suspect for the lack of recovery of Ro, despite the decreasing levels of standard measures of air pollution in California, is the constancy of the very small aerosols that account for the bulk of the CCN concentrations. A major source of very small (<0.1 μm) aerosols, which are as efficient as CCN as are biomass smoke particles, is diesel engines (Lammel and Novakov 1995). A diesel car produces several orders of magnitude more such particles per mile than a gasoline car with the same fuel consumption (Pierson and Brachaczek 1983; Williams et al. 1989; Lowenthal et al. 1994; Weingartner et al. 1997; Maricq et al. 1999). The consumption of diesel fuel in transportation has been increasing in California at 2 times the pace of gasoline consumption since 1980, as has, also, the production of these small CCN aerosols, which are not reflected in any of the standard air-quality measures. Furthermore, these small and numerous particles have the greatest potential for precipitation suppression. In contrast, the larger (>1 μm) pollution particles could actually induce large drops and enhance precipitation, but these particles are the ones that have been most effectively eliminated from the emissions.

e. Classification by synoptic conditions

The next step focused on the cloud types that are most vulnerable to the suppression effects. We expect that most strongly affected would be the clouds forming in the cold sector of the cyclone, because their roots are near the surface so that they can readily ingest the air pollution, as was found by Dayan and Lamb (2003). In addition, the cloud-top temperatures in the cold sector are typically much higher than for the frontal and warm-sector clouds. The roots of the latter clouds are usually not connected directly to the surface, especially in the

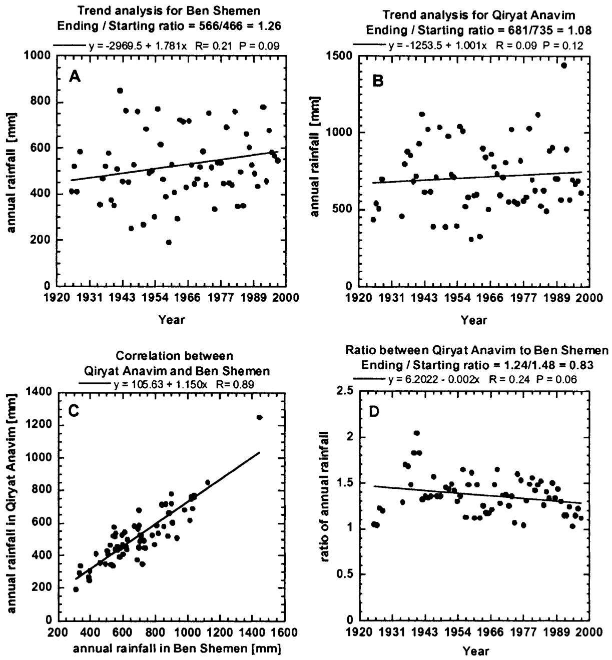

FIG. 4. Same as in Fig. 2, but for a polluted region in Israel, with (a) the lowland station of Ben Shemen and (b) the downwind hilly station of Qiryat Anavim at an elevation of 780 m. (c) The annual rainfall of the two stations is correlated well. Both stations show increases in precipitation over the period of record. (d) Note the decreasing ratio between the two stations with time, as in the urban area in California (Fig. 2).

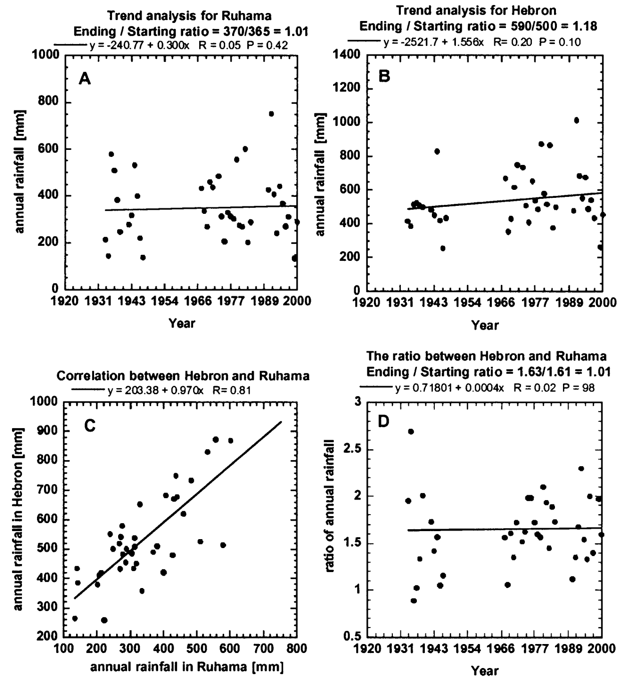

FIG. 5. Same as in Fig. 2, but for a relatively unpolluted region in Israel, with (a) the lowland station of Ruhama and (b) the downwind hilly station of Hebron at an elevation of 1000 m. Rainfall measurements in Hebron are not available for 1944–66. (d) Note the lack of trend in the ratio between the two stations with time, as in the clean area in northern California (Fig. 3).

cold season, but rather feed on long-range transport of moisture. These frontal and warm-sector clouds are forced typically by synoptic lifting, so that their formation is much less dependent on orographic lifting than the clouds in the cold sector, which experience little synoptic forcing. Because all that we had to work with is the radiosonde data, we divided the rain days into ‘‘warm’’ and ‘‘cold’’ classes, delimited at a temperature of -3°C at 700 hPa. This threshold was selected because it is the highest temperature that would still allow convection through that level, starting from a typical winter sea surface temperature of 15°C off the coast of southern California. According to Fig. 7, the orographic enhancement Ro was much greater [by a factor of 5 at the start (S) of the period and a factor of 3.28 at the end (E)] for the clouds in the colder situation. Respectively, Ro for the clouds in the cold conditions showed a strong decrease ($E/S = 3.28/5.00$) in accordance with our conceptual expectations, although it is not statistically significant because of the large scatter. The scatter of the points for the warmer conditions is much smaller, in agreement with the large degree of organization of the frontal and synoptically forced cloud systems versus the poorly organized postfrontal clouds, which is responsible for the large scatter and the lack of statistical significance in the colder conditions. Similar analysis could not be done for Israel because almost all rainfall there occurs from the cold air masses. Nevertheless, this process might explain the large effect in Israel despite the modest height (up to 1 km) of the hills.

f. Trend analyses of mountain snowpack water content

All of the analyses presented up to this point suggest that anthropogenic aerosols suppress the orographic precipitation in stations located at elevations lower than 2 km on the upwind slopes of topographic barriers. The next natural question is, What happens when the clouds are forced across very high barriers and reach very cold temperatures, where aerosols suppress precipitation to a lesser extent because ice precipitation processes become more efficient? The answer was obtained from end-of-winter measurements of the water value of the snowpack near the divide of the Sierra Nevada downwind of Sacramento and Fresno. These data showed only a small (7%–8%) and statistically insignificant decreasing trend of Ro. To make sure that air pollution was still delaying the formation of precipitation in these clouds, the trend of Ro farther upwind and at lower elevations was tested and was found to decrease strongly (22%–24%) and highly significantly (Fig. 8). Similar analysis in pristine areas in northern California showed near-zero to slightly positive trends of Ro at all elevations (see the appendix).

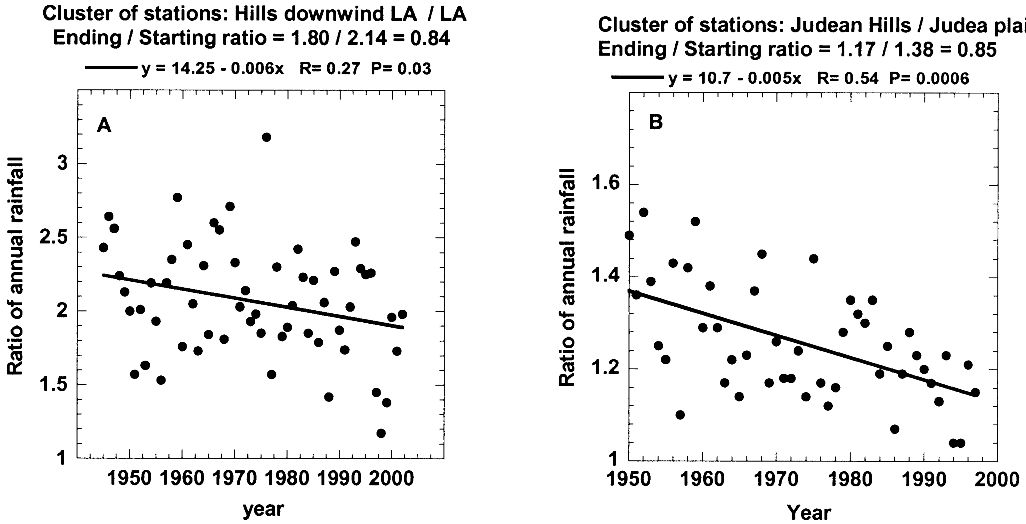

FIG. 6. Recent trends in the annual ratio of precipitation (Ro) between clusters of five–seven gauges in the hills and the upwind urban area of (a) Los Angeles, CA, and (b) the Judean Hills vs the Israel central coastal plain. The small P values show that the trends are statistically significant. Station details are in the appendix.

g. Downslope compensating effects

Next, we explore the question of what happens downwind of the ridgeline to the excess cloud water that was not converted into precipitation because of the suppression of precipitation on the upslope side. It is apparent that the added cloud water and newly formed precipitation particles that pass over the divide cause enhancement of the precipitation on the downslope side. This effect occurs in all areas with available data where suppression was observed on the upslope side—both in California and Israel (see, e.g., Figs. 8, 9). No trends in Ro were found at the upslope or downslope of hills downwind of pristine areas. The opposite trends on the western and eastern slopes downwind of pollution sources are of comparable magnitude in percent, but because the absolute amount of precipitation over the western slope is about 4 times that over the eastern slope (in the case shown in Fig. 9), the net result is dominated by the decrease of Ro over the western (upwind) slopes.

4. Summary of the results

Figures 10, 11, and 12 summarize the results both in California and Israel. Figure 10 displays the trends in Ro in polluted areas downwind of Sacramento, Fresno, and Los Angeles in California and in the Samaria and Judea Hills in Israel. In Fig. 11 it can be seen that no such trend accrued in pristine areas that are located north of San Francisco and in the Hebron Mountains of Israel. Figure 12 shows in a schematic cross section from west to east the full process as it occurs in the polluted mountains of the Sierra Nevada in California (downwind of Fresno). It can be seen that the western slopes are the most sensitive areas to the air-pollution effect. The decrease in the orographic ratio between the plains and the western slopes because of this effect is around 20% (statistically significant). This trend becomes weaker as elevation increases, and the opposite trend occurs in the eastern slopes of the Sierra Nevada. The proportion of the postfrontal precipitation from the colder air masses, which is more orographically controlled (see Fig. 7), has not decreased with time at all, especially at the coastal stations. For example, the fraction of rainfall that occurs with 700-hPa $T < -3°C$, which is associated with the more orographic rainfall, has increased between 1952 and 2000 from 52% to 57% in San Diego while decreasing from 73% to 72% in Cuyamaca (see details in the appendix). This result does not leave any con-

TABLE 1. Concentrations of non–sea salt ions in precipitation at the western slopes of the Sierra Nevada (μeq L^{-1}), and the respective precipitation loss (%) in adjacent rain gauges during the period 1945–2000. The ionic measurements are available from the National Atmospheric Deposition Program (2003). The precipitation Ro changes are provided for Sequoia National Park by the trend in the precipitation ratios of Giant Forest/Fresno, for Yosemite National Park by Pacific House/Sacramento, and for Lassen Volcanic National Park by Lake Spaulin/Ukiah. The full details of the precipitation trend analyses are available in the appendix.

Station	Elev (m)	Period	All record	2001–02	Trend (μeq yr^{-1})	Precipitation Ro change (%)
Sequoia National Park	1902	1981–2002	41.3	35.4	+0.311	−24
Yosemite National Park	1408	1982–2002	30.7	36.5	−0.057	−22
Lassen Volcanic National Park	1765	2001–02	—	17.7	—	0

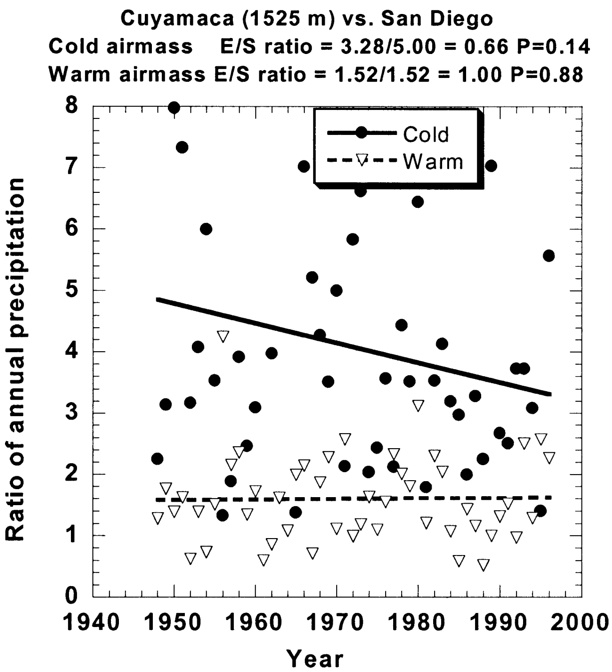

FIG. 7. The annual ratios of precipitation (Ro) between Cuyamaca and San Diego for clouds occurring when $T > -3°C$ at 700 hPa (mainly frontal and warm air mass) and when $T \leq -3°C$ (mainly cyclonic postfrontal clouds).

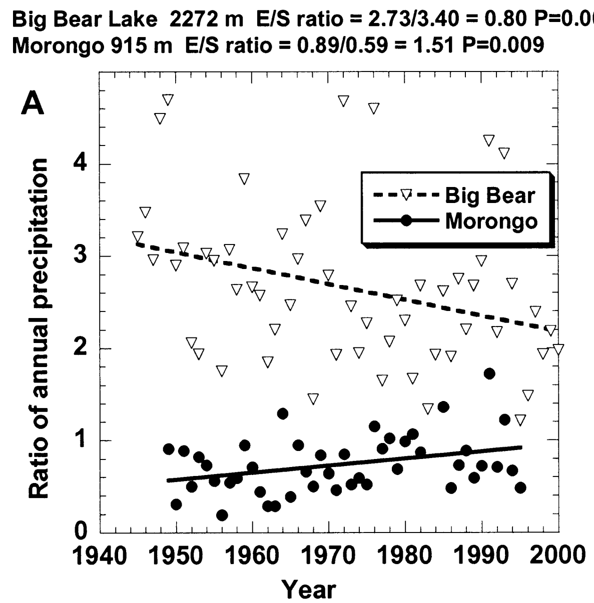

FIG. 9. The annual ratios of precipitation (Ro) of rain gauges on the western slopes (Lake Arrowhead, 1740 m, 1033 mm yr^{-1}, 22C in Fig. 1) and eastern slopes (Morongo, 915 m, 244 mm yr^{-1}, 23C in Fig. 1) of the mountains to the east of Los Angeles with respect to the rainfall in Los Angeles. Note that the decreasing trend on the western slope is coupled with an increasing trend on the eastern slope.

ceivable alternative mechanism of which the authors are aware, except for the aerosol effects that can explain the observed patterns of suppression of the orographic component of the precipitation at the upslope side of the western slopes while increasing it on the eastern slopes.

An important question is the net gain or loss of precipitation along the whole cross section. This is calculated in Table 2 for a 1-km-wide strip across the av-

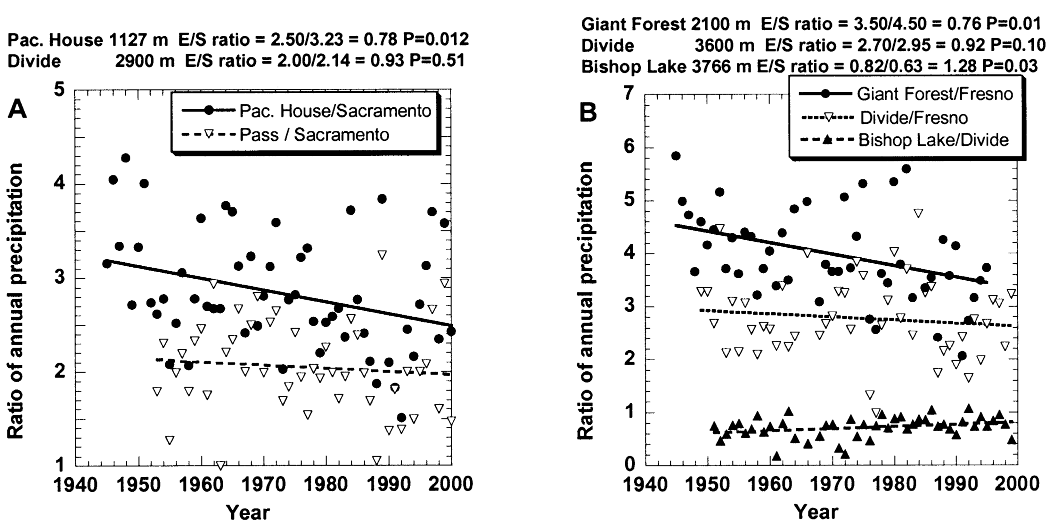

FIG. 8. The annual ratios of precipitation (Ro) between the western slopes of the Sierra Nevada and the upwind lowlands, represented by (a) Pacific House vs Fresno and (b) Giant Forest vs Fresno. The Ro of the water value of the snowpack at the highest western slopes of the Sierra Nevada is represented by an alpine cluster (Sonoma Pass, Bond Pass, Carson Pass) vs (a) Sacramento and the cluster near the divide above Sequoia–Kings Canyon National Park (Mono Pass, Piute Pass, Kaiser Pass, Emerald Lake) vs (b) Fresno. The relative compensation in the eastern slope is shown in (b) by Ro of Bishop Lake with respect to the divide cluster. The locations of the stations in (a) and (b) are shown in the blue frames A and B of Fig. 1 and in Figs. 10a and 10b, respectively.

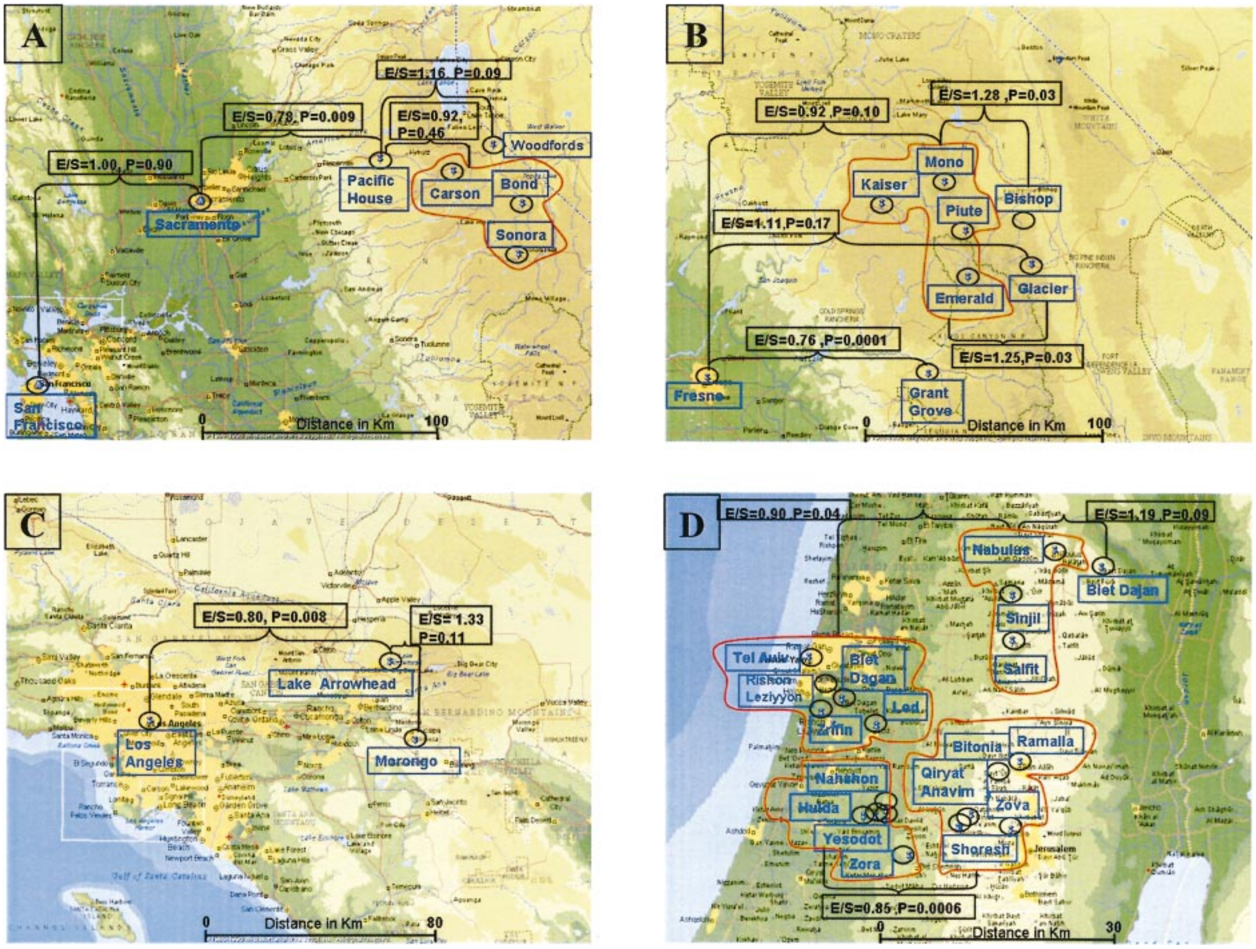

FIG. 10. Summary of trends in precipitation ratios in cross sections downwind of urban areas. (a) The ratios of annual precipitation (Ro) for "polluted" rain gauges at a cross section downwind of Sacramento (6A in Fig. 1) through the Pacific House (1147 m, 1308 mm yr^{-1}) at the western slopes of the Sierra Nevada (7A in Fig. 1), cluster of snowpack stations (2953 m, 945 mm yr^{-1}) at the divide in Alpine County (8A in Fig. 1), and Woodfords (1890 m, 533 mm yr^{-1}) at the eastern slopes of the Sierra Nevada (9A in Fig. 1). (b) Cross section downwind of Fresno (10B in Fig. 1) through Grant Grove (2283 m, 1062 mm yr^{-1}) at the western slopes of the Sierra Nevada (11B in Fig. 1), cluster of snowpack stations (averaging 2953 m, 926 mm yr^{-1}) in Sequoia–Kings Canyon National Park (12B in Fig. 1), Glacier (2733 m, 406 mm yr^{-1}) in the eastern slopes (13B in Fig. 1), and Bishop Lake (3767, 546 mm yr^{-1}) high in the eastern slopes (14B in Fig. 1). (c) Cross section downwind of Los Angeles (19C in Fig. 1) through Lake Arrowhead (1740 m, 1033 mm yr^{-1}) at the western slopes (21C in Fig. 1) and Morongo (915 m, 244 mm yr^{-1}) in the eastern slopes (23C in Fig. 1). (d) Cross section downwind of Tel Aviv area (1D in Fig. 1) through a cluster of stations (660 m, 671 mm yr^{-1}, 2D in Fig. 1) in the Samaria Hills, and Biet Dajan (520 m, 320 mm yr^{-1}, 3D in Fig. 1) in the eastern slopes. It also shows a cross section from a cluster of stations in the Israeli internal plain (180 m, 521 mm yr^{-1}, 7D in Fig. 1) to a cluster of stations in the Judea Hills (743 m, 650 mm yr^{-1}, 6D in Fig. 1).

erage width of the Sierra Nevada stages with their respective rainfall changes as defined in Fig. 12. The reduction in the western slopes dominates the overall hydrological budget, incurring a large net loss of about 20 million m^3 for each 1-km segment of the mountain ranges. This means an overall loss of 4×10^9 m^3 yr^{-1} of precipitation water just for the 200-km-long section of the mountains that are located to the east of the line between Sacramento and Fresno. This calculation is highly oversimplified and provides us merely with the magnitude of the problem. More exact calculations and their hydrological meaning are required. Further, these precipitation losses may not even be evident to water managers because of masking by the long-term increases in the overall upwind base level of precipitation.

In this study, we analyzed only two geographical areas for which we had the physical basis to expect that such unfavorable redistribution of precipitation occurs and for which quality precipitation data at the hilly areas were available to us. Similar effects can be expected in other areas, such as the Snowy Mountains and Victorian Alps in Australia (Rosenfeld 2000), the Atlas Mountains, the Mediterranean coastal hill ranges, Chile, Puerto Rico, and many more locations.

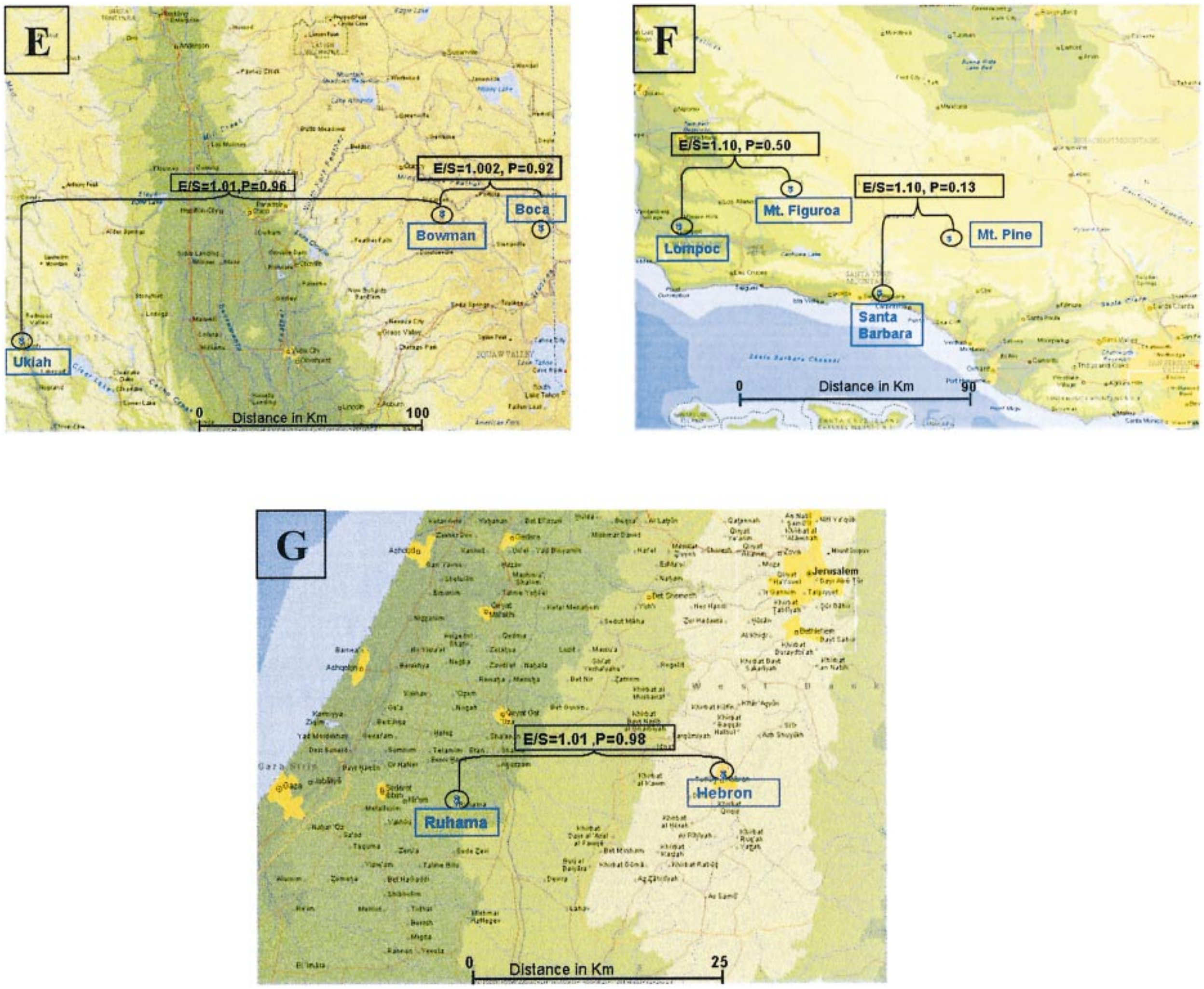

FIG. 11. Same as in Fig. 10, but for a relatively pristine area. (e) Ratios of annual precipitation (Ro) in cross sections downwind of pristine areas in northern California for Ukiah (208 m, 970 mm yr^{-1}, 1E in Fig. 1) through Bowman in the western slopes (2000 m, 1712 mm yr^{-1}, 3E in Fig. 1), to Boca in the eastern slopes (1858 m, 572 mm yr^{-1}, 4E in Fig. 1). (f) Cross section for two pairs of pristine stations to the north of Los Angeles: of Mount Figuroa (1066 m, 508 mm yr^{-1}, 16F in Fig. 1) vs Santa Barbara (33m, 524 mm yr^{-1}, 15F in Fig. 1), and Mount Pine (1400 m, 575 mm yr^{-1}, 18F in Fig. 1) vs Santa Barbara (33 m, 524 mm yr^{-1}, 17F in Fig. 1). (g) Cross section for Hebron (1000 m, 560 mm yr^{-1}, 9G in Fig. 1) in the Hebron Hills vs Ruhama (150 m, 354 mm yr^{-1}, 8G in Fig. 1), which is in Israel's southern plain.

In this study, we avoided addressing the possible confounding effects of the glaciogenic cloud seeding of the orographic clouds that has been taking place in both Israel and California. If seeding did enhance precipitation, the effects in the absence of seeding may have been larger than indicated in this study. Additional research is needed to separate the seeding and pollution effects. In addition, measurements of CCN are needed to strengthen the case for pollution as causal of the apparent losses in precipitation.

5. Conclusions

In summary, strong circumstantial evidence quantitatively links anthropogenic air pollution and the suppression of orographic precipitation downwind of the pollution sources by 15%–25%, in the following ways:

1) The decreasing trend is linked to the period of urbanization and industrialization upwind, whereas similar analysis of the orographic rainfall in nearby pristine areas showed no trends.
2) The suppression occurs mainly in the relatively shallow clouds within the cold air masses of cyclones, which ingest the pollution from the boundary layer while ascending over the mountains.
3) The suppression that occurs over the upslope side is coupled with a similar percentage of enhancement on the much drier downslope side of the hills, prob-

TABLE 2. The approximate budget of precipitation change in the section with suppressed precipitation across the longitudinal zones of the Sierra Nevada, as defined in Fig. 12. The change in precipitated water volume is calculated for a 1-km-wide strip across the mountains.

Zone	Description	Height (m MSL)	Width (km)	Rainfall change (mm yr^{-1})	Rainfall change (m^3)
4	Western slopes	500–2500	100	−220	-22×10^6
5	Divide	>2500	50	−65	-3.25×10^6
6	Eastern slopes	>2000	25	+66	$+1.65 \times 10^6$
Tot					-23.60×10^6

ably because more cloud water passes over the divide.

The main hydrological recharge zones of the water resources in the study areas overlap with the areas for which large and statistically significant suppression of precipitation was measured, with water losses ranging between 15% and 25% of the annual precipitation. The downwind areas in which compensatory enhancement occurs have a much lower absolute amount of precipitation (about 25%) than the upslope side of the hills, and, therefore, the compensatory relative increases on the downwind side are manifested as much smaller amounts of added water when compared with the losses in the upslope areas. For example, a net loss of precipitation water volume of about 4×10^9 is estimated over the mountains to the east of the line connecting Fresno and Sacramento. These are startling results for regions that already now experience severe water shortages and have to resort to seawater desalination (in Israel) to meet their water needs. In addition to the obvious ramifications for water resources, climate impacts are also important and must be considered.

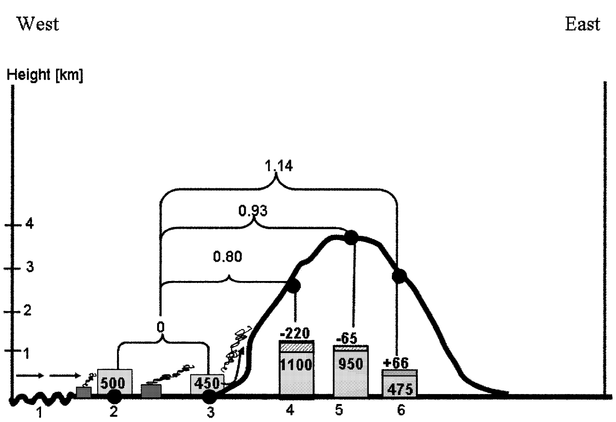

FIG. 12. Topographic cross section showing the effects of urban air pollution on precipitation as the clouds move from west to east from the coast to the Sierra Nevada and to the eastern slopes. The boxes show the amount of the annual precipitation (mm yr^{-1}) in each topographic location, and the numbers above them show the loss or gain of precipitation (mm yr^{-1}) at each site. Maritime air (zone 1) is polluted over coastal urban areas (zones 2, 3), with no decrease in precipitation. The polluted air rises over mountains downwind and forms new polluted clouds (zone 4), with decreases of 15%–20% (losses of 220 mm yr^{-1}) in the ratio between the western slopes and the coastal and plain areas. The clouds reach to the high mountains (zone 5). All of the precipitation is snow, with a slight decrease of 5%–7% (loss of 65 mm yr^{-1}) in the ratio between the summits and the plain areas. The clouds move to the high eastern slopes of the range (zone 6), with an increase of 14% (gain of 66 mm yr^{-1}) in the ratio between the eastern slopes and the plain. According to Table 2, the net loss is dominant.

Acknowledgments. This study was funded by the Israeli Ministry of Science and by the Eshcol Foundation. The authors thank Dr. W. L. Woodley for valuable discussions and for reviewing the manuscript.

APPENDIX

Description of the Additional Tables

This appendix contains additional information about the tables that are presented in this paper. Many more cases and results from California and Israel are discussed here to show that the results that are presented in the article are examples of the general situation. Each of Tables A1–A13 describes different aspects of the discussion, which together help to show the full picture of the time series that we present. The sources for the rain guage data are the National Climatic Data Center, the California Department of Water Resources, and the Israeli Meteorological Service. The names of the stations appear as in the datasets.

The tables contain any of the following information: station name—the rain gauges or snowpack name; lat, lon—the geographical latitude and longitude (in decimal degrees); years—the analyzed period in starting and ending years; elev—the elevation of the rain gauges or snowpacks (m MSL); avg yearly precipitation—the average annual amount of precipitation at each station for the tested years (mm yr^{-1}); correlation—the correlation coefficient between the annual rainfall of pairs of stations; E/S—the ratio (between the precipitation amounts at the hills and at the upwind lowlands) in the end of the time series divided by the ratio in the beginning gives the change, as calculated using the regression line, which is the trend along the years; P value—statistical significance of the trend corresponding to the t-test statistic, which is the probability that the indicated trend occurs because of random variability and is not a real

TABLE A1. Trend analysis for station ratios with no orographic factor.

Station name	San Bernardino	Los Angeles	Sacramento	San Francisco	Cluster of stations in Judea Plains*	Ashdod
Lat, lon (°)	34.160, −117.279	34.053, −118.237	38.583, −121.480	37.783, −122.417	31.746, 34.834	31.500, 34.39
Years	1880–2000		1945–2000		1950–2000	
Elev (m)	366	100	9	17	180	50
Avg yearly precipitation (mm)	394	343	475	538	521	520
Correlation	0.82		0.88		0.88	
E/*S*	1.20/1.19 = 1.01		1.15/1.15 = 1.00		1.02/1.02 = 1.00	
P value	0.82		0.90		0.98	
Slope: 1945–2000	0.0005 (1880–1944)		0.0004		−0.0001	
E/*S*: 1945–74	1.20/1.21 = 0.99 (1880–1944)		1.13/1.15 = 0.98		1.00/1.02 = 0.98 (1950–74)	
P value: 1945–74	0.84 (1880–1944)		0.60		0.72	
Slope: 1945–74	-8×10^{-5} (1880–1944)		−0.002		−0.0015	
E/*S*: 1974–2000	1.20/1.21 = 0.99		1.14/1.09 = 1.04		1.00/1.04 = 0.96	
P value: 1974–2000	0.78		0.36		0.55	
Slope: 1974–2000	−0.006		0.013		−0.008	

* See Table A2 for list of these stations.

TABLE A2. List of stations: cluster of stations in Judea Plains with no orographic factor. Radar observations showed that during post-cold-frontal rain events the orientation of the cloud movement was from west to east, with an average azimuth of 260° (Rosenfeld 1980). It means that the clouds move from the pollution sources in the coast to the Judea and Samaria Mountains and from the relatively clean area in the southern coast to the Hebron Hills.

Station name	Nahshon	Hulda	Zora	Yesodot	Mishmar David
Lat, lon (°)	31.505, 34.574	31.841, 34.909	31.748, 34.959	31.821, 34.834	31.817, 34.898
Elev (m)	200	125	350	70	155
Avg yearly precipitation (mm)	507	536	493	547	486

TABLE A3. Trend analysis for the station ratio: mountain/coastal stations in a clean area.

Station name	Bowman	Fort Bragg	Mount Pine	Santa Barbara	Hebron	Ruhama	Mount Figuroa	Lompoc
Lat, lon (°)	39.613, −120.656	39.613, −123.807	34.609, −119.364	34.417, −119.700	31.320, 35.060	31.301, 34.422	34.736, −120.006	34.663, −120.474
Years	1945–2000		1949–97		1949–97		1949–97	
Elev (m)	2000	27	1400	33	1000	150	1066	40
Avg yearly precipitation (mm)	1712	993	575	524	570	354	508	343
Correlation	0.91		0.89		0.89		0.86	
E/*S*: 1945–2000	1.93/1.80 = 1.07		1.15/1.05 = 1.10 (1949–97)		1.63/1.61 = 1.01 (1949–97)		1.57/1.43 = 1.10	
P value: 1945–2000	0.46		0.13		0.98		0.50	
Slope: 1945–2000	0.010		0.025		0.025		0.002	
E/*S*: 1945–74	1.98/1.84 = 1.07		1.10/1.04 = 1.05 (1949–74)		1.60/1.56 = 1.03 (1994–74)		1.60/1.40 = 1.14 (1994–74)	
P value: 1945–74	0.66		0.63		0.63		0.23	
Slope: 1945–74	0.021		0.015		0.015		0.01	
E/*S*: 1974–2000	2.05/1.79 = 1.14		1.15/1.10 = 1.05		1.67/1.64 = 1.02		1.65/1.58 = 1.04	
P value: 1974–2000	0.44		0.37		0.37		0.78	
Slope: 1974–2000	0.090		0.027		0.027		0.001	
	Lake Spaulding	Ukiah	Mineral	Ukiah	Hemet	El Toro		
Lat, lon (°)	39.319, −120.637	39.150, −123.200	39.350, −116.676	39.150, −123.200	33.699, −116.676	33.600, −117.700		
Years	1895–2000		1930–2000		1896–2000			
Elev (m)	1718	208	1452	208	1452	125		
Avg yearly precipitation (mm)	1822	970	1397	970	499	362		
Correlation	0.87		0.94		0.84			
E/*S*: 1895–2000	1.85/1.85 = 1.00		1.50/1.50 = 1.00 (1945–95)		1.41/1.35 = 1.04			
P value	0.86		0.87		0.55			
Slope	0.0001		−0.0008		0.001			
E/*S*: 1895–1945	1.85/1.85 = 1.00		1.40/1.50 = 0.93 (1945–74)		1.36/1.38 = 0.98			
P value: 1895–1945	0.98		0.47		0.81			
Slope: 1895–1945	0.001		−0.021		0.020			
E/*S*: 1945–2000	1.90/1.85 = 1.03		1.50/1.37 = 1.09		1.46/1.37 = 1.06			
P value: 1945–2000	0.47		0.75		0.34			
Slope: 1945–2000	0.004		0.010		0.007			

TABLE A4. Trend analysis for station ratio: mountain/coastal stations in a polluted area.

Station name	Pacific House	Sacramento	Giant Forest	Fresno	Cluster of mountain stations in Los Angeles area*	Cluster of plains stations in Los Angeles*
Lat, lon (°)	39.613, −120.656	38.583, −121.480	36.568, −118.770	36.770, −119.717	34.215, −117.437	34.013, −118.055
Years	1945–2000		1945–96		1945–2000	
Elev (m)	1147	9	2137	137	1686	107
Avg yearly precipitation (mm)	1308	475	1114	280	890	419
Correlation	0.93		0.86		0.91	
E/*S*: 1945–2000	2.50/3.23 = 0.78		3.50/4.50 = 0.76		1.80/2.14 = 0.84	
P value: 1945–2000	0.009		0.012		**0.03**	
Slope: 1945–2000	0.012		−0.021		−0.006	
E/*S*: 1945–74	2.75/3.20 = 0.85		3.79/4.73 = 0.80		2.15/2.74 = 0.78	
P value: 1945–74	0.11		0.07		0.06	
Slope: 1945–74	−0.030		−0.06		−0.023	
E/*S*: 1975–2000	2.75/2.79 = 0.98		3.35/4.14 = 0.81		1.91/2.23 = 0.85	
P value: 1975–2000	0.84		**0.002**		0.64	
Slope: 1975–2000	−0.008		−0.108		−0.016	

Station name	Cuyamaca	San Diego	Cluster Judea Hills*	Cluster Judea Plains*	Cluster Samaria Hills	Cluster central coast*
Lat, lon (°)	32.983, −116.583	32.733, −117.133	31.825, 35.128	31.746, 34.834	32.171, 35.208	31.982, 34.826
Years	1880–2000		1950–96		1952–96	
Elev (m)	1550	123	743	180	660	39
Avg yearly precipitation (mm)	875	290	650	521	671	551
Correlation	0.83		0.96		0.91	
E/*S*: 1880–2000	3.27/4.53 = 0.72 (1880–2000)		1.17/1.38 = 0.85		1.10/1.20 = 0.90	
P value: 1880–2000	**0.003** (1880–2000)		**0.0006**		**0.04**	
Slope: 1888–2000	−0.0009 (1880–2000)		−0.010		−0.005	
E/*S*: 1945–74	3.50/4.00 = 0.87		1.21/1.36 = 0.89 (1950–74)		1.14/1.20 = 0.95 (1952–72)	
P value: 1945–74	0.10		**0.03**		0.26	
Slope: 1945–74	−0.0186		0.0053		0.0053	
E/*S*: 1975–2000	3.24/3.62 = 0.89		1.15/1.28 = 0.89 (1975–96)		1.07/1.20 = 0.89	
P value: 1975–2000	0.07		**0.01**		0.17	
Slope: 1975–2000	−0.040		−0.020		−0.006	

TABLE A4. (*Continued*)

Station name	Mount Hamilton	San Francisco	Grant Grove	Fresno
Lat, lon (°)	37.333, −121.650	37.783, −122.417	36.568, −118.770	36.770, −119.717
Years	1882–2000		1945–96	
Elev (m)	1402	175	2193	137
Avg yearly precipitation (mm)	670	538	1061	280
Correlation	0.75		0.86	
E/*S*: 1880–2000	1.07/1.54 = 0.70		3.49/4.60 = 0.76	
P value: 1880–2000	**0.0002**		**0.0001**	
Slope: 1880–2000	−0.005			
E/*S*: 1945–74	1.00/1.59 = 0.63		4.00/4.60 = 0.86	
P value: 1945–74	**0.00006**		0.07	
Slope: 1945–74	−0.015		−0.015	
E/*S*: 1975–2000	1.12/1.14 = 0.98		3.00/4.14 = 0.72	
P value: 1975–2000	0.80		**0.002**	
Slope: 1975–2000	−0.005		−0.043	

* See Table A5 for a list of the stations.

TABLE A5. Trends analysis for station ratios in a polluted area in California. Each mountain station is against the cluster of plains stations in Los Angeles.

Trends of mountain stations

Station name	Lake Arrowhead	Sierra PH	Big Bear Dam	Crystal 28	Cender Sp
Lat, lon (°)	34.25, −117.187	34.200, −117.246	34.242, −116.975	34.327, −117.837	34.356, −117.876
Elev (m)	1740	1000	2272	1923	2260
Avg yearly precipitation (mm)	1033	781	876	882	722
E/*S*: 1945–2000	2.51/3.17 = 0.80	2.04/2.31 = 0.88	1.76/2.36 = 0.75	2.36/2.68 = 0.88	2.00/2.60 = 0.77
P value: 1945–2000	**0.008**	0.17	**0.001**	**0.04**	**0.05**
Slope: 1945–2000	−0.027	−0.012	−0.027	−0.028	−0.012
E/*S*: 1945–74	2.42/3.50 = 0.73	1.82/2.26 = 0.80	2.40/3.07 = 0.78	2.00/2.57 = 0.78	1.81/2.41 = 0.76
P value: 1945–74	**0.02**	0.11	**0.03**	0.16	**0.01**
Slope: 1945–74	−0.083	−0.038	−0.083	−0.036	−0.021
E/*S*: 1974–2000	1.50/1.59 = 0.94	2.10/2.19 = 0.96	1.80/2.02 = 0.89	2.20/2.46 = 0.89	1.86/2.00 = 0.93
P value: 1974–2000	0.67	0.79	0.50	0.65	0.62
Slope: 1974–2000	−0.022	−0.007	−0.022	−0.016	−0.013

List of the cluster of coastal and plains stations

Station name	Los Angeles 355	Los Angeles CC	Los Angeles AP	Pomona	Beverly Hills 22	Long Beach 224	San Bernardino
Lat, lon (°)	34.087, −118.095	34.050, −118.233	33.942, −118.387	34.067, −117.817	34.074, −118.399	33.768, −118.191	34.104, −117.268
Elev (m)	103	93	35	25	85	60	347
Avg yearly precipitation (mm)	393	373	325	416	426	290	421

TABLE A6. Trend analysis for polluted stations in Israel. Each mountain station is against the cluster of Judea Plains stations.

Judea Hills/Judea Plains

Trend analysis of the individual stations of the Judea Hills cluster

Station name	Qiryat Anavim	Shoresh	Zova	Biet Meir
Lat, lon (°)	31.813, 35.121	31.800, 35.066	31.796, 35.178	31.79, 35.046
Elev (m)	780	680	730	530
Avg yearly precipitation (mm)	685	605	640	625
E/*S*: 1950–96	1.29/1.46 = 0.88	1.20/1.32 = 0.91 (1956–96)	1.16/1.36 = 0.85	1.14/1.29 = 0.88
P value: 1950–96	**0.01**	0.24	**0.02**	**0.003**
Slope: 1950–96	−0.0036	−0.002	−0.0042	−0.003
E/*S*: 1950–74	1.31/1.48 = 0.89	1.18/1.32 = 0.89	1.22/1.34 = 0.91	1.22/1.28 = 0.95
P value: 1950–74	0.11	**0.009**	0.19	0.49
Slope: 1950–74	−0.0076	−0.11	−0.004	−0.002
E/*S*: 1975–96	1.22/1.49 = 0.82	1.16/1.40 = 0.83	1.07/1.37 = 0.78	1.11/1.25 = 0.88
P value: 1974–97	**0.006**	0.09	**0.03**	**0.002**
Slope: 1974–97	−0.011	−0.011	0.015	−0.005

Station name	Ramalla	Bitonia
Lat, lon (°)	31.899, 35.197	31.855, 35.163
Elev (m)	870	800
Avg yearly precipitation (mm)	707	653
E/*S*: 1952–96	1.09/1.41 = 0.77	1.17/1.32 = 0.88
P value: 1952–96	**0.01**	0.08
Slope: 1952–96	−0.009	−0.0028
E/*S*: 1952–74	1.20/1.46 = 0.82	1.29/1.26 = 1.02
P value: 1950–74	0.17	0.47
Slope: 1952–74	−0.013	0.0027
E/*S*: 1950–96	1.05/1.31 = 0.80	1.10/1.30 = 0.85
P value: 1975–96	0.06	**0.04**
Slope: 1975–96	−0.011	−0.009

List of Judea Plains stations

Station name	Nahshon	Hulda	Zora	Yesodot	Mishmar David
Lat, lon (°)	31.505, 34.574	31.841, 34.909	31.748, 34.959	31.821, 34.834	31.817, 34.898
Elev (m)	200	125	350	70	155
Avg yearly precipitation (mm)	507	536	493	547	486

Samaria Hills/Central Coast

Trend analysis of mountain stations

Station name	Nablus	Sinjil	Salfit
Lat, lon (°)	32.225, 35.268	32.161, 35.173	32.086, 35.184
Elev (m)	680	775	520
Avg yearly precipitation (mm)	651	657	707
E/*S*: 1952–96	1.05/1.20 = 0.88	1.08/1.20 = 0.88	1.12/1.20 = 0.93
P value; 1952–96	**0.04**	0.17	0.49
Slope: 1952–96	−0.0038	−0.0028	0.0038
E/*S*: 1952–96	1.09/1.27 = 0.86	1.10/1.30 = 0.85	1.20/1.18 = 1.02
P value: 1952–96	0.14	0.16	0.52
Slope: 1952–96	−0.0098	−0.014	0.0047
E/*S*: 1952–96	1.03/1.17 = 0.88	1.06/1.19 = 0.89	1.11/1.34 = 0.83
P value: 1952–96	0.23	0.29	0.07
Slope: 1952–96	−0.005	−0.008	−0.011

List of central coast stations

Station name	Tel Aviv	Bet Dagan	Lod	Rishon-Leziyyon	Zrifin
Lat, lon (°)	32.059, 34.761	31.996, 34.830	31.954, 34.897	31.958, 34.810	31.946, 34.833
Elev (m)	25	30	50	50	60
Avg yearly precipitation (mm)	551	555	570	522	560

TABLE A7. Trend analysis for station ratios: snowpack water content vs coastal stations in a ''clean'' area.

Station name	Mount Lassen	Fort Bragg	Mount Shasta	Ukiah
Lat, lon (°)	40.281, −121.303	39.623, −123.807	41.717, −122.383	39.150, −123.200
Years	1945–2000		1930–2000	
Elev (m)	2750	27	2633	200
Avg yearly precipitation (mm)	2032	991	1355	970
Correlation	0.85		0.90	
E/*S*: 1945–2000	2.20/2.04 = 1.08		1.36/1.28 = 1.09	
P value: 1945–2000	0.41		0.18	
Slope: 1945–2000	0.006		0.006	
E/*S*: 1945–74	2.15/2.00 = 1.07		1.35/1.29 = 1.11	
P value: 1945–74	0.42		0.26	
Slope: 1945–74	0.011		0.010	
E/*S*: 1974–2000	2.21/2.00 = 1.10		1.50/1.29 = 1.16	
P value: 1974–2000	0.56		0.19	
Slope: 1974–2000	0.018		0.022	

TABLE A8. Trend analysis for station ratios: cluster of snowpack water content vs coastal stations in California in polluted areas.

Station name	Cluster of mountain stations in Alpine County, CA*	Sacramento	Cluster of mountain stations in Sequoia–Kings Canyon NationalPark, CA*	Fresno
Lat, lon (°)	38.880, −119.442	38.583, −121.480	37.173, −118.735	36.770, −119.719
Years	1948–2000		1951–2000	
Elev	2953	8	3537	137
Avg yearly precipitation (mm)	945	475	900	280
Correlation	0.85		0.85	
E/*S*: 1948–2000	2.00/2.14 = 0.93		3.17/3.42 = 0.92	
P value: 1948–2000	0.46		0.10	
Slope: 1948–2000	−0.017		−0.015	
E/*S*: 1948–74	1.83/2.09 = 0.88		3.20/3.34 = 0.95	
P value: 1948–74	0.38		0.80	
Slope: 1948–74	0.022		−0.010	
E/*S*: 1975–2000	1.80/1.82 = 0.98		2.93/3.25 = 0.92	
P value: 1975–2000	0.97		0.42	
Slope: 1975–2000	−0.001		−0.033	

* See Table 9 for list of stations.

TABLE A9. Trend analysis of snowpack water content stations in California in a polluted area.

Station name	Stations in Alpine County vs Sacramento: Sonoma Pass	Bond Pass	Carson Pass
Lat, lon (°)	38.417, −119.59	38.327, −119.373	38.188, −119.363
Elev (m)	2833	3100	2933
Avg yearly precipitation (mm)	889	1085	630
E/*S*: 1945–2000	1.25/1.39 = 0.90	2.33/2.33 = 1.00	1.80/2.05 = 0.89
P value: 1948–2000	0.30	0.76	0.25
Slope: 1948–2000	−0.008	−0.004	−0.013
E/*S*: 1945–74	1.45/1.45 = 1.00	2.67/2.25 = 1.18	2.04/2.00 = 1.02
P value: 1948–74	0.47	0.23	0.85
Slope: 1948–74	0.017	0.035	0.005
E/*S*: 1974–2000	1.20/1.41 = 0.85	1.36/1.11 = 1.11	2.00/2.02 = 0.99
P value: 1974–2000	0.35	0.53	0.78
Slope: 1974–2000	−0.024	0.030	−0.001

Station name	Stations in Sequoia–Kings Canyon National Park: Mono Pass	Piute Pass	Kaiser Pass	Emerald Lake
Lat, lon (°)	37.263, −118.463	37.144, −118.412	37.176, −119.609	37.110, −118.457
Elev (m)	3817	3767	3033	3533
Avg yearly precipitation (mm)	780	910	985	885
E/*S*: 1945–2000	3.30/3.22 = 1.03	3.25/3.39 = 0.96	3.41/3.66 = 0.93	2.70/2.95 = 0.93
P value: 1945–2000	0.91	0.75	0.77	**0.03**
Slope: 1945–2000	0.006	−0.006	−0.016	−0.126
E/*S*: 1945–74	3.28/2.79 = 1.17	3.24/3.37 = 0.96	3.67/3.60 = 1.02	3.10/2.75 = 1.12
P value: 1945–74	0.79	0.86	0.94	0.44
Slope: 1945–74	0.042	−0.008	0.005	0.027
E/*S*: 1974–2000	2.88/3.08 = 0.94	3.10/3.56 = 0.87	3.30/3.60 = 0.91	2.70/2.70 = 1.00
P value: 1974–2000	0.67	0.56	0.73	0.94
Slope: 1974–2000	−0.050	−0.451	−0.037	0.012

TABLE A10. Trend analysis for station ratios: mountain/coastal stations on eastern slopes in a clean area.

Station name	Boca	Bowman
Lat, lon (°)	39.388, −120.080	38.583, −120.656
Years	1945–2000	
Elev (m)	1858	2000
Avg yearly precipitation (mm)	572	1711
Correlation	0.88	
E/*S*: 1945–2000	3.02/3.00 = 1.002	
P value: 1945–2000	0.92	
Slope: 1945–2000	0.010	
E/*S*: 1945–74	0.75	
P value: 1945–74	3.00/3.00 = 1.00	
Slope: 1945–74	0.003	
E/*S*: 1975–2000	3.00/3.00 = 1.00	
P value: 1975–2000	0.68	
Slope: 1975–2000	0.017	

TABLE A11. Trend analysis for stations ratio: east slope/west slope stations in a polluted area.

Station name	Woodfords	Pacific House	Glacier	Grant Grove	Morongo	Los Angeles International Airport	Biet Dajan	Samaria Hills Cluster*	Bishop Lake	Fresno	Bishop Lake	Cluster of mountain stations downwind of Fresno area**
Lat, lon (°)	38.776, −119.820	38.750, −120.500	37.126, −118.433	36.741, −118.961	33.921, −117.173	33.942, −118.387	32.201, 35.364	32.224, 35.268	37.123, −118.545	36.741, 18.961	37.740, −118.326	37.488, −119.442
Years	1945–2000		1945–2000		1948–96		1960–96		1951–2000		1951–2000	
Elev (m)	1890	1147	2733	2283	915	37	520	660	3767	2283	3767	3537
Avg yearly precipitation (mm)	533	1321	406	1067	244	330	434	671	545	1067	550	900
Correlation	0.86		0.86		0.70		0.88		0.84		0.89	
E/*S*: 1945–2000	0.44/0.38 = 1.16		0.48/0.38 = 1.25		0.89/0.67 = 1.33		0.67/0.56 = 1.19		2.13/1.80 = 1.18		0.82/0.63 = 1.28	
P value: 1945–2000	0.09		**0.03**		0.11		0.09		0.28		**0.03**	
Slope: 1945–2000	0.003		0.007		0.006		0.0026		0.018		0.005	
E/*S*: 1945–74	0.44/0.40 = 1.10 (1974–90)		0.45/0.33 = 1.33		0.80/0.67 = 1.19 (1949–73)		Missing data		1.90/1.84 = 1.03		0.60/0.69 = 0.88	
P value: 1945–74	**0.04**		**0.01**		0.38		Missing data		0.82		0.41	
Slope: 1945–74	0.005		0.014		0.003		Missing data		0.010		−0.008	
E/*S*: 1975–2000	0.40/0.43 = 0.94		0.42/0.45 = 0.93		0.89/0.95 = 0.94 (1974–95)		0.66/0.60 = 1.08 (1968–94)		2.14/2.00 = 1.07		0.86/0.77 = 1.12	
P value: 1975–2000	0.15		0.46		0.42		0.44		0.26		0.28	
Slope: 1975–2000	−0.010		−0.004		−0.0007		0.005		0.025		0.010	

* See Table A6 for list of stations.
** See Table A8 for list of stations.

TABLE A12. Trend analysis for individual rain stations.

Station name	Cuyamaca	San Diego	Lake Spaulding	Ukiah	San Francisco	Mount Hamilton
Lat, lon (°)	32.983, −116.583	32.730, −117.180	39.319, −120.367	39.150, −123.200	37.780, −122.420	37.330, −121.650
Elev (m)	1550	123	1717	2833	175	1407
Avg yearly precipitation (mm)	875	290	1692	208	538	595
E/*S* precipitation: 1888–2000	0.980/992 = 0.90 (1888–2000)	256/254 = 1.01 (1888–2000)	1765/1584 = 1.11 (1895–1945)	980/901 = 1.09 (1895–1945)	521/500 = 1.04	540/741 = 0.72
P value: 1888–2000	0.14	0.50	0.14	0.20	0.73	**0.0001**
Slope: 1888–2000	−0.143	0.190	0.479	0.983	0.016	−0.224
E/*S* precipitation: 1888–1945	980/970 = 1.01	271/281 = 0.96	1535/1717 = 0.90	820/967 = 0.85	507/532 = 0.95	629/772 = 0.82
P value: 1888–1945	0.64	0.63	0.21	0.27	0.65	**0.02**
Slope: 1888–1945	0.005	0.015	−0.529	−0.277	−0.050	−0.315
E/*S* precipitation: 1945–2000	931/808 = 1.15	290/220 = 1.32	1981/1686 = 1.17	1029/906 = 1.13	587/447 = 1.31	609/540 = 1.12
P value: 1945–2000	0.39	**0.03**	0.14	0.23	0.57	0.12
Slope: 1945–2000	0.100	0.126	0.720	0.310	0.247	0.103

Station name	Ben Shemen	Kiryat Anavim	Fresno	Giant Forest	Bishop Lake	Cluster of mountain stations downwind of the Fresno area
Lat, lon (°)	31.921, 34.834	31.800, 35.121	36.770, −119.717	36.770, −118.770	37.123, −118.545	37.488, −119.442
Elev	100	780	137	2137	3767	3537
Avg yearly precipitation (mm)	586	685	280	1114	546	900
E/*S*: precipitation: 1945–2000	600/500 = 1.20 (1925–2000)	735/637 = 1.13 (1925–2000)	308/244 = 1.26	1057/980 = 1.08	595/490 = 1.21	762/718 = 1.06
P value: 1945–2000	0.11	0.13	0.10	0.80	0.15	0.62
Slope: 1945–2000	1.570	1.600	0.055	0.080	0.300	0.133

Station name	Sacramento	Pacific House	Cluster of mountain stations in Alpine County	Big Bear Lake	Morongo	
Lat, lon (°)	38.583, −121.480	39.613, −120.656	37.173, −118.735	34.242, −117.173	3.921, −116.975	
Elev (m)	9	1147	3537	2272	915	
Avg yearly precipitation (mm)	475	1308	890	890	244	
E/*S*: precipitation: 1945–2000	432/533 = 1.23	1361/1270 = 1.07	1016/940 = 1.08	838/925 = 0.91	184/307 = 1.67 (1949–96)	
P value: 1945–2000	0.11	0.75	0.39	0.56	0.13	
Slope: 1945–2000	0.230	0.113	0.240	−0.189	0.239	

Station name	Hebron	Ruhama	Cluster Judea Hills	Cluster Judea Plains	Cluster of mountain stations in Los Angeles area	Cluster of plains stations in Los Angeles
Lat, lon (°)	31.320, 35.060	31.301, 34.422	31.825, 35.128	31.746, 34.834	34.215, −117.437	34.010, −118.055
Elev (m)	1000	150	743	180	1686	107
Avg yearly precipitation (mm)	560	354	650	521	890	381
E/*S* precipitation: 1945–2000	600/513 = 1.16 (1934–96)	370/318 = 1.16 (1934–96)	657/600 = 1.09 (1950–96)	590/487 = 1.20 (1950–96)	787/735 = 1.07	419/333 = 1.24
P value: 1945–2000	0.36	0.28	0.46	0.07	0.19	0.06
Slope: 1945–2000	2.194	0.890	1.702	2.558	0.176	1.638

TABLE A13. Trend analysis for individual rain stations during cold (T at 700 hPa $\leq -3°C$) and warm ($T > -3°C$) air mass.

Radiosonde site	San Diego		Los Angeles	
Station name	San Diego	Cuyamaca	Los Angeles	Lake Arrowhead
Lat, lon (°)	32.733, −117.133	32.983, −116.583	34.050, −118.095	34.250, −117.187
Elev (m)	123	1550	35	1740
Avg yearly precipitation (mm)	290	875	373	1033
E/S precipitation, warm sector (mm day^{-1})				
1952–2000	16.0/12.7 = 1.26	25.0/20.2 = 1.24	23.0/23.2 = 0.99	19.3/17.8 = 1.08
P value: 1952–2000	**0.02**	0.08	0.89	0.67
Slope: 1952–2000	0.153	0.101	−0.042	0.060
E/S: precipitation, cold sector (mm day^{-1})				
1952–2000	20.8/13.5 = 1.54	65.5/55.0 = 1.18	29.1/20.2 = 1.43	36.8/30.0 = 1.20
P value: 1952–2000	**0.02**	0.46	**0.01**	0.17
Slope: 1952–2000	0.159	0.102	0.147	0.020

trend (values $\leq$ 0.05 are boldfaced to highlight their significances); E/S precipitation—same as E/S, but for individual rain gauge time series, not pairs of station ratios; cluster—groups of rain gauges or snowpacks that represent the average annual precipitation in a selected geographical area.

REFERENCES

Alpert, P., and H. Shafir, 1991: On the role of the wind vector interaction with high-resolution topography in orographic rainfall modeling. *Quart. J. Roy. Meteor. Soc.,* **117,** 421–426.

Borys, R. D., D. H. Lowenthal, S. A. Cohn, and W. O. J. Brown, 2003: Mountain and radar measurements of anthropogenic aerosol effects on snow growth and snowfall rate. *Geophys. Res. Lett.,* **30,** 1538, doi:10.1029/2002GL016855.

Carroll, J. J., and A. J. Dixon, 2002: Regional scale transport over complex terrain, a case study: Tracing the Sacramento plume in the Sierra Nevada of California. *Atmos. Environ.,* **36,** 3745–3758.

Changnon, S. A., 1979: Rainfall changes in summer caused by St. Louis. *Science,* **205,** 402–404.

——, R. T. Shealy, and R. W. Scott, 1991: Precipitation changes in fall, winter, and spring caused by St. Louis. *J. Appl. Meteor.,* **30,** 126–134.

Collett, J. L., Jr., 1989: Characterization of cloud water and precipitation chemistry and deposition at elevated sites in central and southern California. Ph.D Thesis, California Institute of Technology, 317 pp.

——, B. Daube Jr., J. W. Munger, and M. R. Hoffmann, 1989: Cloudwater chemistry in Sequoia National Park. *Atmos. Environ.,* **23,** 999–1007.

——, ——, and M. R. Hoffmann, 1990: The chemical composition of intercepted cloudwater in the Sierra Nevada. *Atmos. Environ.,* **24A,** 959–972.

Dayan, U., and D. Lamb, 2003: Meteorological indicators of summer precipitation chemistry in central Pennsylvania. *Atmos. Environ.,* **37,** 1045–1055.

Lammel, G., and T. Novakov, 1995: Water nucleation properties of carbon black and diesel soot particles. *Atmos. Environ.,* **29,** 813–823.

Lowenthal, D. H., B. Zielnska, J. C. Chow, J. G. Watson, M. Gautam, D. H. Ferguson, G. R. Neuroth, and K. D. Stevens, 1994: Characterization of heavy-duty diesel vehicle emissions. *Atmos. Environ.,* **28,** 731–743.

Malm, W. C., B. A. Schichtel, and R. B. Ames, 2002: A 10-year spatial and temporal trend of sulfate across the United States. *J. Geophys. Res.,* **107,** 4627, doi:10.1029/2002JD002107.

Maricq, M. M., R. E. Chase, D. H. Podsiadlik, and R. Vogt, 1999: Vehicle exhaust particle size distributions: A comparison of tailpipe and dilution tunnel measurements. Society of Automotive Engineers Tech. Paper 1999-01-1462, 30 pp.

National Atmospheric Deposition Program, cited 2003: NTN sites in CA. [Available online at http://nadp.sws.uiuc.edu/sites/sitemap.asp?state=CA.]

Neiman, J. N., P. J. Ralph, A. B. White, D. E. Kingsmill, and P. O. G. Persson, 2002: The statistical relationship between upslope flow and rainfall in California's coastal mountains: Observations during CALJET. *Mon. Wea. Rev.,* **130,** 1468–1492.

Pandey, G. R., D. R. Cayan, and K. P. Georgaakakos, 1999: Precipitation structure in the Sierra Nevada of California during winter. *J. Geophys. Res.,* **104,** 12 019–12 030.

Pierson, W. R., and W. W. Brachaczek, 1983: Particulate matter associated with vehicles on the road II. *Aerosol Sci. Technol.,* **2,** 1–40.

Rosenfeld, D., 1980: Characteristics of rainfall cloud systems, radar and satellite images over Israel. M.S. thesis, Department of Atmospheric Sciences, Hebrew University, 127 pp.

——, 1999: TRMM observed first direct evidence of smoke from forest fires inhibiting rainfall. *Geophys. Res. Lett.,* **26,** 3105–3108.

——, 2000: Suppression of rain and snow by urban air pollution. *Science,* **287,** 1793–1796.

——, and H. Farbstein, 1992: Possible influence of desert dust on seedability of clouds in Israel. *J. Appl. Meteor.,* **31,** 722–731.

——, and W. L. Woodley, 2003: Closing the 50-year circle: From cloud seeding to space and back to climate change through precipitation physics. *Cloud Systems, Hurricanes, and the Tropical Rainfall Measuring Mission, Meteor. Monogr.,* No. 51, Amer. Meteor. Soc., 59–80.

Shepherd, J. M., H. Pierce, and A. J. Negri, 2002: Rainfall modification by major urban areas: Observations from spaceborne rain radar on the TRMM satellite. *J. Appl. Meteor.,* **41,** 689–701.

Takemoto, B. K., and Coauthors, 1995: Acidic deposition in California: Findings from a program of monitoring and effects research. *Water Air Soil Pollut.,* **85,** 261–272.

Weingartner, E., H. Burtscher, and U. Baltensperger, 1997: Hygroscopic properties of carbon and diesel soot particles. *Atmos. Environ.,* **31,** 2311–2327.

Williams, D. J., J. W. Milne, S. M. Quigley, and D. B. Roberts, 1989: Particulate-emissions from in-use motor vehicles. *Atmos. Environ.,* **23,** 2647–2661.